Effects of substrate temperature on the structure and photoelectrical properties of ZnO films prepared via sputtering

XIAOLING FAN[a,b], JUNCHENG LIU[a*], SHENQIU ZHAI[a], RUI DING[a]

[a]*School of Materials Science and Engineering, Shandong University of Technology, Zibo 255049*
[b]*Department of Engineering Glass, Jin Jing Group Co. LT., Zibo 255086*

ZnO thin films were prepared using radio frequency (RF) magnetron sputtering from a ZnO ceramic target. The effects of the substrate temperature on the ZnO thin film structure, surface morphology and photoelectrical properties were investigated. The ZnO films were all composed of polycrystalline grains with hexagonal wurtzite structures and a c-axis preference. With an increase in the substrate temperature, the c-axis preference of the ZnO thin film crystal grain was more obvious, and the grain size increased slightly; the granule size, consisting of many grains, also increased. More importantly, the granule's outline changed from a sheet to spherical; the film's inner stress changed from compressive to tensile. The film's carrier concentration increased by nearly three orders of magnitude, whereas its Hall mobility decreased fourfold. The film's resistivity decreased by more than two orders of magnitude as the substrate temperature increased from 25 to 600 °C. Although the thin film transmittance decreased slightly with an increase in the substrate temperature, all of the films exhibited high transmittances that averaged 85% in the visible region (400~800 nm). Additionally, the optical band gap for the ZnO thin films also decreased slightly and ranged from 3.28 to 3.26 eV.

1. Introduction

Research into direct wide band gap semiconductor materials has attracted much more attention due to the huge market demand of blue and violet light-emitting devices or lasers. Zinc oxide (ZnO) is currently considered a very promising material for bright ultraviolet and blue optical devices, such as light-emitting diodes (LED), laser diodes (LD), and photodiodes (PD), because of its interesting characteristics, including its large direct band gap of 3.37 eV at room temperature and its large exaction binding energy of 60 meV, which is 2.4 times greater than that of GaN [1]. Furthermore, this material is also widely used in transparent conductive contacts, thin-film gas sensors, varistors, solar cells, and other devices.

To obtain high-quality ZnO films, various advanced techniques have been used to prepared the film, such as sputtering [1], chemical vapor deposition (CVD) [2], the sol–gel method [3], the spray pyrolysis technique [4], pulse laser deposition (PLD) [5], metal-organic chemical vapor deposition (MOCVD) [6] and molecular beam epitaxial (MBE) [7]. Compared with other techniques, sputtering has a few of advantages, such as simple equipment requirements, a high deposition rate, a low substrate temperature, a good surface flatness, transparency and dense layer formation, and nearly zero hazard materials discharge. The ZnO film characteristics are generally affected by the preparation conditions, such as the substrate types and temperature, the deposition method, and the working pressure [8]. The substrate temperature

affects the migration rate of the atoms adsorbed by the surface and the re-evaporation and crystallization of the film grains, which changes the film structure and properties [9].

Kim et al. [10] deposited Ga-doped ZnO (GZO)/ZnO bi-layered films on glass substrates by radio frequency magnetron sputtering at different substrate temperatures of 100, 200 and 300 °C. The film's lowest resistivity of 2.7×10^{-3} Ω·cm was observed for films deposited at 300 °C. The result means that increasing the substrate temperature enhanced the optical transmittance and electrical conductivity of GZO/ZnO bi-layered films, simultaneously. Zhu et al. [11] deposited Al and Ga co-doped zinc oxide (AGZO) thin films on glass substrates by DC magnetron sputtering under different substrate temperatures. The average grain size increased from 20.6 nm to 51.4 nm with substrate temperatures ranging from 150 to 450 °C. The carrier concentration, Hall mobility of the thin films increased when the substrate temperature increased from 150 to 350 °C, and then decreased with a further increase of substrate temperature. The film deposited at 350 °C exhibited a lowest resistivity of 3.0×10^{-4} Ω·cm with the highest carrier concentration of 5.0×10^{20} cm^{-3} and Hall mobility of 42 cm^{2}V^{-1}s^{-1}. Siva et al. [12] investigated the effect of substrate heating on nano-composite ZnO-SiO$_x$ thin films grown by RF co-sputter deposition. With increase of substrate temperature, ZnO nanocrystals grow with better UV absorption, lower defects, and better crystalline quality and migrate from surface to subsurface regions of the film, but the content and crystalline quality

of Zn_2SiO_4 phase increases. The results show that the substrate temperature can be used to control the content and crystalline quality of ZnO and Zn_xSiO_y phases in the films and hence tune them for different applications. Huang et al. [13] prepared transparent conducting oxide films of boron and gallium co-doped ZnO (BGZO) on glass substrates by radio frequency magnetron sputtering at room temperature and 200°C, respectively. With the increase thickness and substrate temperature, the grain size of BGZO films increased and the full width at half maximum decreased, the carrier mobility increased and the resistivity decreased, which indicated that the crystallinity and conductivity of films improved. And the optical band gap of BGZO thin films decreased with the substrate temperature increase. Swart et al. [14] investigated the effects of the substrate temperature and the post annealing temperature on ZnO:ZnPLD thin film properties. They found that the crystallite sizes were 19 nm, 25 nm and 39 nm, while the average particles sizes were 95 nm, 85 nm and 129 nm for the film deposited at 50 °C, 200 °C and 400 °C respectively. The crystallite sizes and particles sizes seemed to increase with the increase in the substrate temperature. Oh et al. [15] had a detailed study about the substrate temperature dependence in the ZnO films grown on (001) GaAs substrates using RF sputtering. A series of ZnO films are prepared in the substrate temperature range of room temperature to 500 °C. The photoluminescence intensity ratio of near-band edge and deep level in the ZnO films decreased with the increase of substrate temperature, which is ascribed to the interdiffusion of Zn and As atoms and the formation of various chemical states in the ZnO/GaAs heterointerface. Tao et al. [16] prepared Mo-doped ZnO (MZO) transparent conductive thin films on glass substrate under various substrate temperatures from 50 °C to 200 °C. They found that the film's resistivity decreased acutely, but both the mobility and the carrier concentration increased firstly then decreased with the substrate temperature increase. And the lowest resistivity was obtained to be 2.8×10^{-3} $\Omega \cdot cm$. Wang et al. [17] prepared undoped and Cu-doped ZnO (ZnO:Cu) thin films using magnetron co-sputtering. Higher substrate temperature enhances the crystallinity and reduces the compressive stress of the films. Both Cu-doping and increasing substrate temperature lead to rougher surface and larger granules. The resistivity of both the ZnO and ZnO:Cu films increases with the substrate temperature. Interestingly, the optical band gap Eg of ZnO:Cu films increases significantly with the substrate temperature, while Eg of the undoped film is not obviously influenced. Mahdhi et al. [18] prepared transparent conducting thin films of ZnO:Ga (GZO) on glass substrates by RF magnetron sputtering from nano-particles synthesized by the sol–gel method. The substrate temperature ranged from room temperature to 300°C. The results revealed that the film's resistivity decreased acutely, though both the mobility and the carrier concentration increased firstly then decreased with the substrate temperature increase. Thin films of GZO have a low resistivity, with a minimum value of 2.20×10^{-3} $\Omega \cdot cm$ deposited at a substrate temperature of 200 °C.

In this work, undoped ZnO thin films were prepared using RF magnetron sputtering from a pure ZnO ceramic target in a pure Ar atmosphere. The effects of the substrate temperature on the ZnO film structure and properties were investigated.

2. Experimental

ZnO films were prepared on SiO_2 substrates using an RF-magnetron sputtering process in a 99.999% pure Ar atmosphere using a ZnO ceramic target as the starting material (99.99% purity, Φ76×3 mm), a target-to-substrate distance of approximately 55 mm, and a sputtering time of 50 min. The background pressure in the sputtering chamber was 6.0×10^{-4} Pa, the RF power was 100 W, and the working pressure was 1.0 Pa. The substrate was cleaned with de-ionized water, ethanol, toluene, and acetone in an ultrasonic bath and was cleaned again with pre-sputtering 10 minutes before deposition. The substrate temperature was set at 25 °C, 400 °C, and 600 °C.

The film's crystalline structure was characterized using X-ray diffraction (XRD, D8 Advance with Cu Kα1 radiation, λ= 0.15406 nm). The surface morphology was observed using scanning electron microscopy (SEM, Multimode NS3a). The optical properties were measured using a UV-vis spectrophotometer (775 PC) over a wavelength range of 200 to 800 nm. The film thickness was measured with an SGC-10 optical thin-film measurement system. The Hall effects were tested using an HMS-3000 in a dark room to exclude unwanted ambient light.

3. Results and discussions

3.1. Effect of the substrate temperature on the film's crystal structure

Fig. 1 shows the XRD patterns of the ZnO films prepared under different conditions. There were four peaks at 29.016°, 34.095°, 36.250°, and 68.230° at 25 °C, which were indexed to the (100), (002), (101), and (112) polycrystalline characteristic peaks of ZnO, respectively. There were also four peaks at 31.711°, 34.377°, 36.169°, and 62.515° in the 400℃ pattern, which were indexed to the (100), (002), (101), and (103) polycrystalline characteristic peaks of ZnO, respectively. However, there was only one peak at 34.437° at 600℃, which was indexed to the (002) characteristic peak of polycrystalline ZnO. For all patterns, the (002) peak was significantly more intense than the other peaks, such as those for (100), (101), and (102). This result indicated that hexagonal ZnO polycrystals with c-axis `preferential` orientation formed to create the film. Moreover, the (002) peak rapidly increased, whereas the other peaks decreased as the temperature increased, which meant that the film was of the highest crystallization at 600 °C.
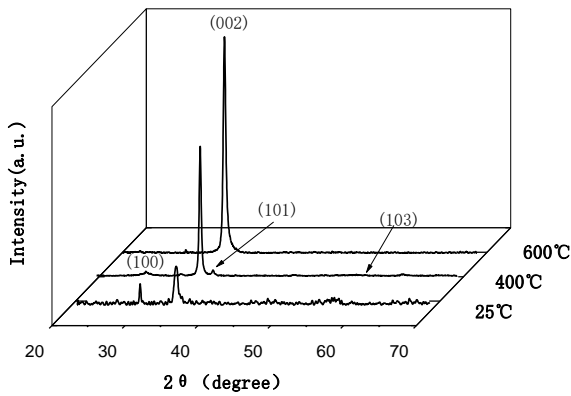
Fig. 1. Effect of the substrate temperature on the XRD patterns of the films

The crystallite size can be estimated from the full-width at half maximum (FWHM) of the (002) peak in the XRD pattern using the Debye-Scherrer formula:

$$D = 0.9\lambda/(\beta\cos\theta) \quad (1)$$

where λ is the X-ray wavelength, θ is the Bragg diffraction angle, and β is the FWHM for the (002) diffraction peak [19]. The stress in the film plane was calculated using the following relation:

$$\sigma = [2C^2_{13}-(C_{11}+C_{12})C_{33}/C_{13}] (c_0-c)/C_{13}c_0 = -233 (c_0-c)/c_0 \quad (2)$$

where the elastic constant, C_{ij}, takes the data for a ZnO single crystal: $C_{11}=208.8$, $C_{33}=213.8$, $C_{12}=119.7$ and $C_{13}=104.2$ GPa; c is the lattice constant that is twice the interplanar spacing for the hexagonal crystal system ZnO, i.e., $c=2d$, $c_0 =2d_0$ for a standard ZnO powder (2.603 Å ·2=0.5206 nm, JCPDS 36-1451), and c for the ZnO film determined via XRD. A negative stress for σ indicates that the film is under compression, whereas a positive stress denotes a tensile state [19]. The calculated stress and grain size are shown in Table 1.

It is clear from Table 1 that as the substrate temperature increased, the 2θ angle for the (002) plane diffraction peak moved from 34.095° to 34.437°, the interplanar spacing decreased from 2.627 Å to 2.602 Å, the diffraction peak FWHM decreased from 0.459° to 0.413°, and the crystallite size increased from 18.5 nm to 20.7 nm. Meanwhile, the value of the inner stress in the film decreased significantly and became a tiny positive value from a large negative value, i.e., the compressive stress became tensile. This is because the interplanar spacing for the film with the substrate at 600 °C was closest to, but already less than, d_0 for the standard ZnO powder. All of the results above confirmed again that the ZnO film crystallization improved with an increase in substrate temperature.

When the substrate was at a low temperature, the diffusion and migration abilities of the ions or atoms in the grains were very limited due to their low energy, and their realignment was very difficult; therefore, the preferential (002) orientation of the crystallization was inhibited to a large extent. With an increase in the substrate temperature, the diffusion and migration abilities of the ions were enhanced, so the preferential crystallization (002) orientation became more and more significant, and the other diffraction peaks almost disappeared. Meanwhile, this type of migration and realignment also resulted in stress relief and grain growth [20, 21].

Table 1 The structural parameters of the films

Substrate temperature (°C)	2θ (°)	d (Å)	β (°)	D (nm)	σ (GPa)
25℃	34.095	2.627	0.459	18.5	-2.418
400℃	34.377	2.606	0.431	19.8	-1.398
600℃	34.437	2.602	0.413	20.7	0.0895
ZnO standard powder	34.43	2.603			

3.2. Effect of the substrate temperature on the film's surface morphology

The SEM images in Fig. 2 show the morphologies for the film surfaces. All of the films are rather compact. The granules in Fig. 2 (a) appear as thin sheets with irregular contours that have a size ranging from approximately 10 nm to 200 nm. Many tiny granules fill between the larger granules such that the granule outline and interface among the granules are not so clear. The granules in Fig. 2 (b) appear as thick sheets with round contours with sizes ranging from approximately 20 nm to 200 nm. Additionally, the amount of the tiny granules that are filled among the larger granules is reduced such that the granule outline and interface among the granules are very clear. In Fig. 2(c), the granules nearly appear as balls with sizes ranging from approximately 20 nm to 200 nm, and the amount of tiny granules is further reduced.
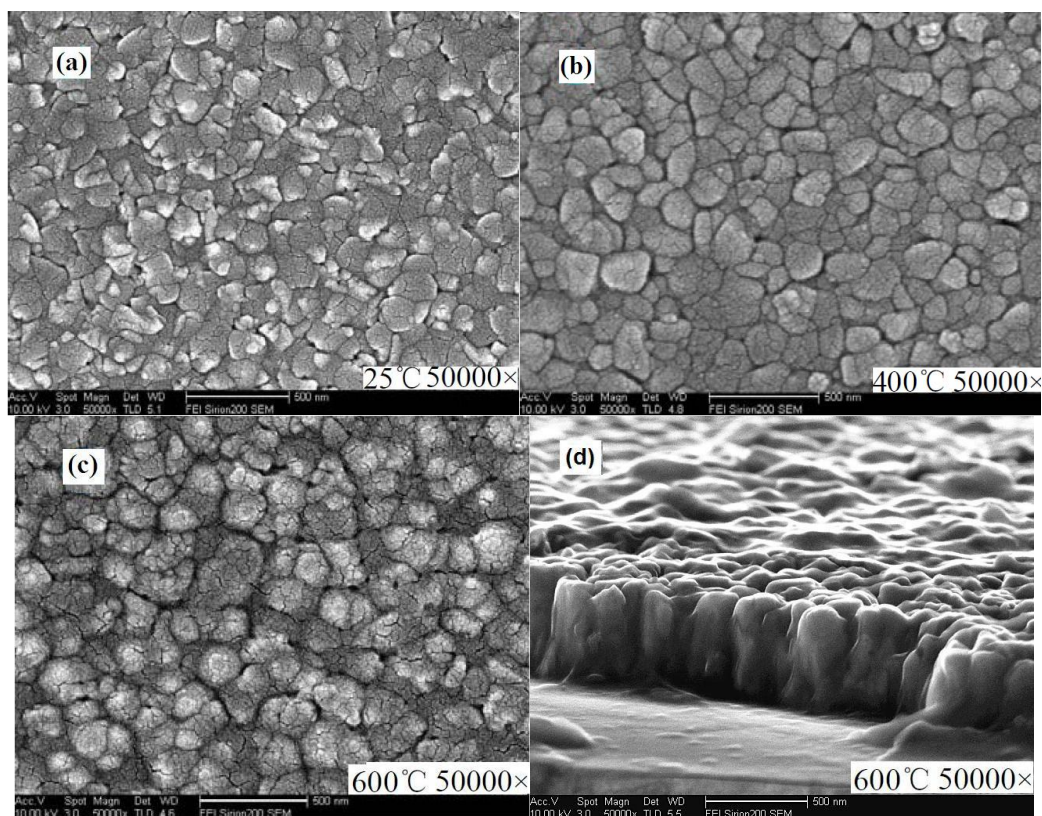
Fig. 2. Effect of the substrate temperature on the ZnO film surface morphology

In general, the size of the granules composing of the film increased, and their outline involved from sheet to spherical with the substrate temperature increase, seen from Fig. 2(a) to 2(c). Fig. 2(d), a cross-sectional SEM image, may show the granules' outline more clearly, of which upper sections are just like spherical crowns. Moreover, the film's thickness is estimated to be about 350 nm, which is a little greater than the values ranging from 250 nm to 300 nm measured with SGC-10 optical thin-film measurement system. One possible reason is that the shooting angle for Fig. 2(d) was a little tilted, not just perpendicular to the film's cross section.

Furthermore, the average granule size in Fig. 2 is significantly greater than the corresponding crystallite in Table 1 calculated from the Debye-Scherrer formula. A larger granule should be an aggregate of many crystallites. Swart et al. [14] had a similar result, the crystallite sizes were 19 nm, 25 nm and 39 nm, while the average particles sizes were 95 nm, 85 nm and 129 nm for the film deposited at 50 °C, 200 °C and 400 °C respectively. The crystallite sizes and particles sizes seemed to increase with the increase in the substrate temperature. As the substrate temperature increased, the diffusion and migration abilities not only of the ions in the grains but also of the atoms and molecules clinging to the film growth surface were enhanced. Therefore, it was difficult for a tiny granule to be created on the film growth surface. Even if a tiny granule was created, it would easily dissolve into a larger one, i.e., the granule would be swallowed by a larger one. In other words, the increase in the substrate temperature promoted the merging of neighboring grains or granules

and hindered the formation of the new nuclei or granules, and the average grain or granule size increased [20, 21]. In fact, the grain or the granule growth, their merging, and their contour glomeration were driven by the interface energy and the whole free energy decrease from the thermodynamics, whereas a high temperature only provided sufficient dynamic conditions.

3.3. Effect of the substrate temperature on the electrical properties of the film

Fig. 3 shows the resistivity, ρ, the carrier concentration, n, and the Hall mobility, μ, for the films obtained using a Hall-effect meter.

Increasing the substrate temperature increased the carrier concentration first slowly (from 25 to 400 °C) and then rapidly (from 400 to 600 °C), which resulted in a nearly three orders of magnitude increase in total. In contrast, increasing the substrate temperature decreased both the body resistance and the Hall mobility in a manner that was initially rapid (from 25 to 400 °C) and then slow (from 400 to 600 °C). The resistivity decreased by more than two orders of magnitude, and the Hall mobility decreased fourfold in total.
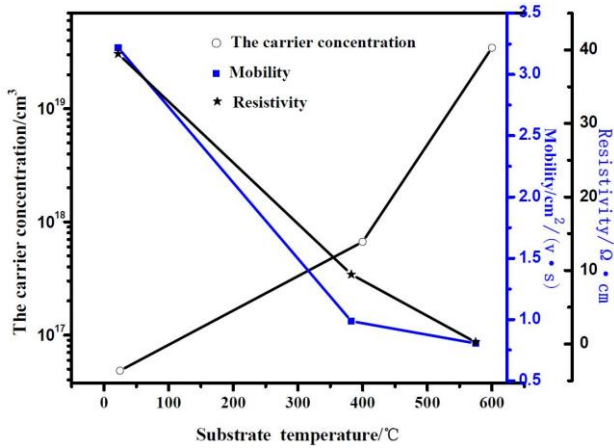
Fig. 3 Effect of the substrate temperature on the ZnO
film electrical properties

Fig. 4. Effect of the substrate temperature on the ZnO film
optical transmission spectra

3.4. Effect of the substrate temperature on the film optical property

For the polycrystalline ZnO film, the electron mobility, μ_n, could be expressed by the following formula [15]:

$$\frac{1}{\mu_n} = \frac{1}{\mu_l} + \frac{1}{\mu_i} + \frac{1}{\mu_G} \qquad (3)$$

where μ_l, μ_i, and μ_G stand for the lattice scattering mobility, ionized impurity scattering mobility, and the grain boundary scattering mobility, respectively.

The substrate temperature increase improved the film crystallinity and increased the crystal grain size and the granule size. Therefore, both the lattice scattering and the grain boundary scattering should be depressed, and μ_l, and μ_G should increase, and then, μ_n should increase. Conversely, the equilibrium vapor pressure of the oxygen atom in ZnO is greater than that of the zinc atom. As the high substrate temperature promoted the dissociation of the oxygen atom from the ZnO, the donor (oxygen vacancy) concentration increased significantly, and the collision probability between the carrier and the donor increased, and the ionized impurity scattering was enhanced, so the carrier mobility decreased [22]. The actual measured carrier mobility decreased with the increase in the substrate temperature, which indicates that the ionized impurity scattering mobility has played a dominant role.

The resistivity, ρ, could be expressed by the following formula: $\rho = 1/nq\mu_n$, where n is the carrier concentration. For the polycrystalline ZnO film, the carrier concentration primarily depends on the oxygen vacancy concentration [23]. As the substrate temperature increased, the carrier concentration increased by nearly three orders of magnitude in total, and the mobility decreased by only fourfold in total; therefore, the resistivity decreased by more than two orders of magnitude.

The optical transmission spectra for the ZnO films at room temperature are shown in Fig. 4. All of the spectra present obvious wave troughs and crests in the visible light range due to the interference effect. The film's optical transmission decreased significantly when the substrate's temperature increased. The increase in the substrate temperature improved the film crystallinity, which reduced the scattering and absorption of the crystal lattice and the grain boundary to the visible light and improved the film's optical transmission. Conversely, the substrate temperature increased the oxygen vacancy concentration more significantly, which, thus, enhanced the scattering and absorption of the visible light greatly and reduced the film's optical transmission. The actual transmission decrease indicated that the latter effect exceeded the former effect. However, all of the films were highly transparent in general, with an average transmission of 85% in the visible range, and their spectral curves exhibited sharp fundamental absorption edges corresponding to their respective band gaps. These results indicate that every film has excellent functional ultraviolet absorption.

The band gap of a semiconductor material is not only an important theoretical problem in condensed matter physics but also a fundamental parameter for the design of semiconductor devices. The band gap is primarily determined by the material's atomic composition and bonding state but also by the impurities and defects. The following relationship is used to determine the energy band gap, E_g, for a direct transition semiconductor [24]:

$$\alpha h v = A(h v - E_g)^{1/2}$$

Where h is Planck's constant and v is the incident photon frequency; $\alpha = -\ln T_R/t$, T_R is the transmitted light intensity, t is the ZnO film thickness. Eg can be obtained from a plot of $(\alpha h v)^2$ versus the photon energy, $h v$, which was extrapolated to the energy axis in the spectrum using a straight line. The band gap of the film, Eg, ranged from 3.26 to 3.28 eV, as shown in Fig. 5. These values are less than the intrinsic ZnO band gap of 3.37 eV. A possible reason for this result is that the shallow donor or deep acceptor energy levels formed by the defects in the ZnO thin film decreased the optical band gap [8]. Additionally,

the inner stress in the film may also reduce the optical band gap [25].
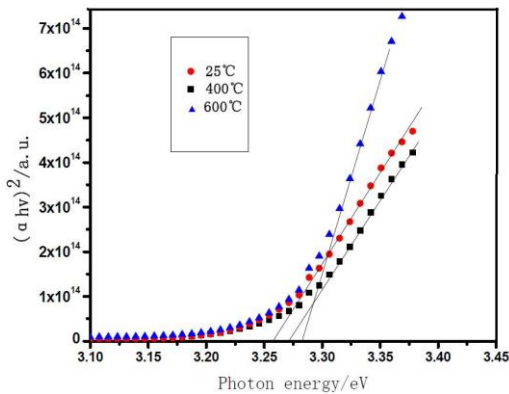
Fig. 5. Effect of the substrate temperature on the ZnO film band gap

4. Conclusions

ZnO thin films were prepared using radio frequency magnetron sputtering from a ZnO ceramic target. The effects of the substrate temperature on the ZnO thin film structure, surface morphology and photoelectrical properties were investigated.

The ZnO films were all composed of polycrystalline grains with hexagonal wurtzite structures and a c-axis preference. When the substrate temperature increased, the c-axis preference of the ZnO thin film crystal grain was more obvious, and the grain size increased slightly; the granule size, which consisted of many grains, also increased. More importantly, the granule outline changed from a sheet form to a spherical form. Moreover, the film's inner stress changed from compressive to tensile.

As the substrate temperature increased, the film's carrier concentration increased by nearly three orders of magnitude, whereas the Hall mobility decreased fourfold and the resistivity decreased by more than two orders of magnitude.

Although the thin film transmittance decreased slightly with an increase in the substrate temperature, all films exhibited high transmittances averaging 85% in the visible region (400~800 nm). The optical band gap for the ZnO thin films also decreased slightly and ranged from 3.28 eV to 3.26 eV.

Acknowledgements

References

[1] N. E. Duygulu, A. O. Kodolbas, A. Ekerim, J. Cryst. Growth **381**, 51 (2013).

[2] S. Chen, G. Carraro, D. Barreca, R. Binions, Thin Solid Films **584**, 316 (2015).

[3] S. Chen, M. E. A. Warwick, R. Binions, Sol. Energy Mater. Sol. Cells **137**, 202 (2015).

[4] Y. Aoun, B. Benhaoua, S. Benramache, B. Gasm, Optik **126**, 2481 (2015),

[5] C. Cachoncinlle, C. Hebert, J. Perrière, M. Nistor, A. Petit, E. Millon, App. Surf. Sci. **336**, 103 (2015)

[6] A. Fouzri, M.A. Boukadhaba, A. Touré, N. Sakly, A. Bchetnia, V. Sallet, Appl. Surf. Sci. **311**, 648 (2014)

[7] M. Ying, W. Cheng, X. Wang, B. Liao, X. Zhang, Z. Mei, X. Du, Mater. Lett. **144**, 12 (2015).

[8] T. Liu, X. Fei, L. Hu, H. Zhang, Y. Li, S. Duo, Superlattice Microst. **83**, 604 (2015).

[9] Y. Liu, H. Liu, W. Li, Q. Zhao, Y. Qi, Acta Physico-Chimica Sinica **29**, 631 (2013).

[10] S. –K. Kim , S. –H. Kim, S. –Y. Kim, J. –H. Jeon, T. –K. Gong, D. –H. Choi, D. -I Son, D. Kim, Ceram. Int. **40**, 6673 (2014)

[11] K. Zhu, Y. Yang, W. Song, Mater. Lett. **145**, 279 (2015)

[12] V. V. Siva Kumar, D. Kanjilal, J. Alloys Compd. **639**, 511 (2015)

[13] J. Yang, J. Huang, Y. X. Lu, H. H. Ji, L. Zhang, K. Tang, M. Cao, Y. Hu, L. J. Wang, Surf. Eng. **33**, 270 (2016)

[14] E. Hasabeldaim, O. M. Ntwaeaborwa, R. E. Kroon, E. Coetsee, H. C. Swart, Opt. Mater., article in press,   DOI: 10.1016/j.optmat.2017.03.027;

[15] Soo-Man Lee, Kang-Bok Kim, Hang-Ju Ko, Dong-Cheo Oh, J. Nanoelectron Optoe. **11**, 250 (2016).

[16] G. Chen, X. Zhao, H. Zhang, H. Wang, F. Liu, X. Zhang, J. Gao, Y. Zhao, C. Zhang, J. Tao, Mat. Sci. Eng. B-Adv. **211**, 135 (2016)

[17] P. Zhou, H. Liu, L. Zhang, X. Suo, Z. Liang, Y. Liu, Y. Li, Z. Jiang, Z. Wang, J. Mater. Sci.-Mater. El. **27**, 7822 (2016)

[18] H. Mahdhi, Z. Ben Ayadi, J. L. Gauffier, K. Djessas, J. Electron. Mater. **45**, 557 (2016)

[19] Y. G. Wang, S. P. Lau, H. W. Lee, S. F. Yu, B. K. Tay, X. H. Zhang, K. Y. Tse, H. H. Hng, J. Appl. Phys. **94**, 1597 (2003).

[20] C. Z. Wang, Z. Chen, Y. He, Appl. Surf. Sci. **15**, 6881 (2009).

[21] X. Zhang, S. Ma, F. Li, F. Yang, J. Liu, Q. Zhao, J. Alloy Compd. **574**, 149 (2013).

[22] J. Wang, C. Li, W. Niu, Semiconductor devices physics, Science Press, 1983, Beijing.

[23] X. Li, M. Zhu, Y. Hou, B. Wang, H. Yan, Piezoelectrics & Acoustooptics **26**, 318 (2004).

[24] B. L. Zhu, J. Wang, S. J. Zhu, J. Wu, D. W. Zeng, C. S. Xie, Thin Solid Films **520**, 6963 (2012).

[25] B. Liu, Y. Zhou, H. Zheng, M. Li, Z. Guo, Q. Zhao, Y. Peng, Rare Metals **30**, 170 (2011)

---

*Corresponding author: jchliu@sdut.edu.cn